ESI for

Trapped Copper in [6]Cycloparaphenylene: a Fully-Exposed Cu_7 Single Cluster for Highly Active and Selective CO Electro-Reduction

Yi-Qing Liu, Zi-Yang Qiu, Xiang Zhao, Wei-Wei Wang, Jing-Shuang Dang

Content

Computational Methods

The periodic density functional theory (DFT) calculations were performed by using the Vienna ab initio simulation program (VASP.5.4.4)[1-3] along with the spin-polarized Perdew-Burke-Ernzerhof (PBE)[4] functional.

The Cu(111) slab model was composed of a 5 × 5 × 5 unit cell (a = b = 10.2754 Å, c = 20.4873 Å, α = β = 90 °， γ = 120 °) with a vacuum set to 12.23 Å in the z-direction. The bottom three layers of the slab were fixed during geometry optimization. Calculations on the Cu_7@[6]CPP were also represented by a periodic model constructed using bulk cell dimensions: a = b = c = 20.60 Å, α = β = γ = 90 °. The repeated units were separated from their neighboring molecules by a 16.34 Å vacuum in the c-direction.

A plane-wave cut off energy of 500 eV was used and the convergence tolerances for the force were set as 0.02 eV/Å and 10^{-5} eV for the energy, respectively. The 3 × 3 × 1 and 1 × 1 × 1 Monkhorst–Pack k-point meshes were adopted to sample the surface Brillouin zone of Cu(111) and Cu_7@[6]CPP-involving structures, respectively.[5] In the cases of Cu(111)-involving structures, the bottom three layers of the slab were fixed in optimization and all the five Cu layers were fixed in frequency calculations. As for the Cu_7@[6]CPP-involving structures, all the atoms were allowed to relax during optimization and frequency calculations. Kinetically, the climbing image nudged elastic band method (CI-NEB) approach was used to locate transition states with 7 images and frequency analyses were carried out to confirm the nature of saddle points.

The computational hydrogen electrode (CHE) model was used to calculate Gibbs free energy change (ΔG) for each elemental step， as pioneered by Nørskov and co-workers.[6-7] ΔG was calculated as

$$\Delta G = \Delta E + \Delta E_{ZPE} - T\Delta S + eU + \Delta G_{pH}$$

where ΔE is the reaction energy, ΔE_{ZPE} and ΔS are zero-point energy and entropy change at T = 298.15 K, respectively. ΔG_{pH} is the free energy correction of pH, which is obtained by $\Delta G_{pH} = k_B T \times \ln 10 \times$ pH, and pH = 0 was assumed in the present study. e and U refer to the number of electrons transferred and the applied electrode potential, respectively. Moreover, the free energy of the proton-electron pair was used as one-half of the chemical potential of the hydrogen molecule.

In addition, we also employed an approximate solvation correction proposed by Nørskov and co-workers to account for the effect of water.[7-8] The Gibbs free energies of *OH, *CO, *CHO, and *R-OH intermediates are stabilized by 0.5, 0.1, 0.1, and 0.25 eV, respectively. Moreover, for the limiting potential step (*CO→*CHO) of the CRR process, we introduced an implicit solvent model for the optimizations of *CO and *CHO, in which the code of VASPsol[9] was used with a dielectric constant of 78.54 to simulate the H_2O solvent environment. We found the calculated $\Delta G_{CO\text{-}CHO}$ by employing those two approaches are almost same (0.40 eV and 0.39 eV), and accordingly, to reduce computational cost, the empirical solvation correction was used to calculate the free energy changes.

[1] G. Kresse, J. Furthmüller, *Phys. Rev. B* **1996**, *54*, 11169-11186.

[2] G. Kresse, J. Hafner, *Phys. Rev. B* **1993**, *47*, 558-561.

[3] G. Kresse, J. Hafner, *Phys. Rev. B* **1994**, *49*, 14251-14269.

[4] J. P. Perdew, K. Burke, M. Ernzerhof, *Phys. Rev. Lett.* **1996**, *77*, 3865-3868.

[5] H. J. Monkhorst, J. D. Pack, *Phys. Rev. B* **1976**, *13*, 5188-5192.

[6] J. K. Nørskov, J. Rossmeisl, A. Logadottir, L. Lindqvist, J. R. Kitchin, T. Bligaard, H. Jónsson, *J.*

Phys. Chem. B **2004**, *108*, 17886-17892.

[7] A. A. Peterson, F. Abild-Pedersen, F. Studt, J. Rossmeisl, J. K. Nørskov, *Energy Environ. Sci.* **2010**, *3*, 1311-1315.

[8] W. J. Durand, A. A. Peterson, F. Studt, F. Abild-Pedersen, J. K. Nørskov, *Surf. Sci.* **2011**, *605*, 1354-1359.

[9] K. Mathew, R. Sundararaman, K. Letchworth-Weaver, T. A. Arias, R. G. Hennig, *J. Chem. Phys*. **2014**, *140*, 084106.

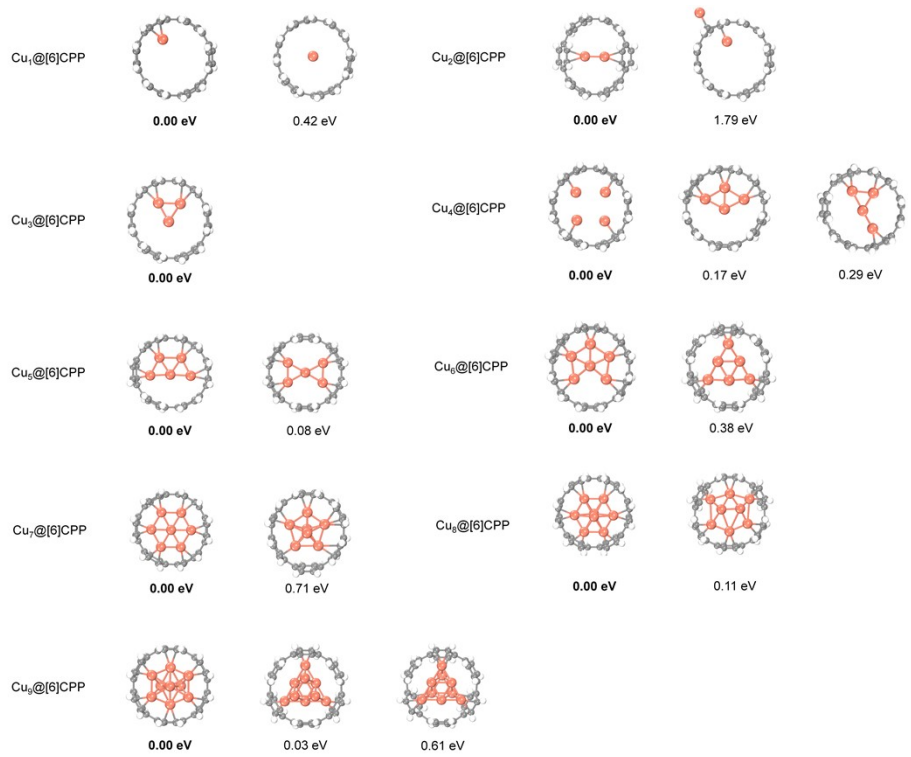

Figure S1. All optimized structures of Cu_n@[6]CPP (n = 1-9) with the relative energies corresponding to the most stable isomer of each series.

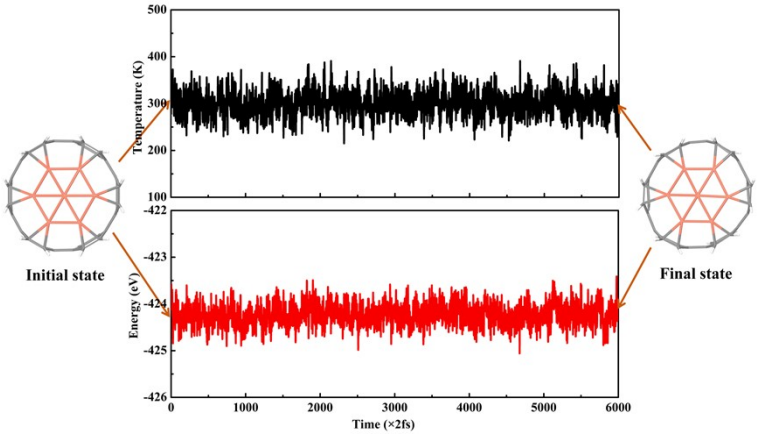

Figure S2. AIMD simulations of Cu_7@[6]CPP at room temperature.

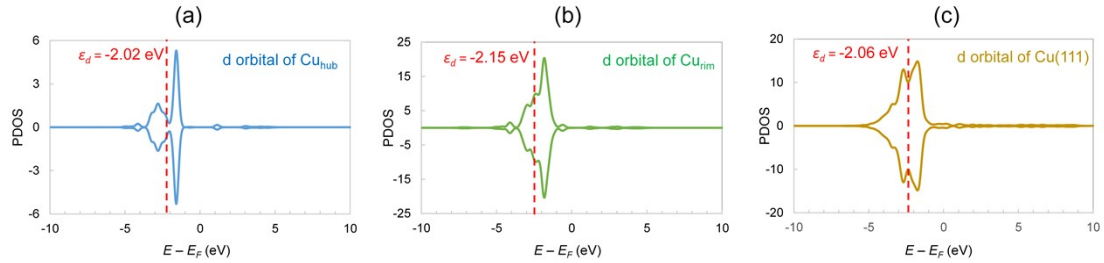

Figure S3. Projected densities of states (PDOS) of the d orbital and the d-band center (ε_d) of Cu_{hub} and Cu_{rim} of Cu_7@[6]CPP and a Cu_7 fragment of Cu(111) surface. The Fermi level (E_F) is set to zero.

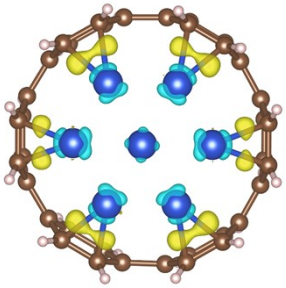

Figure S4. Charge density difference of Cu_7@[6]CPP. Yellow and cyan denote charge accumulation and depletion, respectively. The isosurface value is set to 0.008 e/Å^3 .

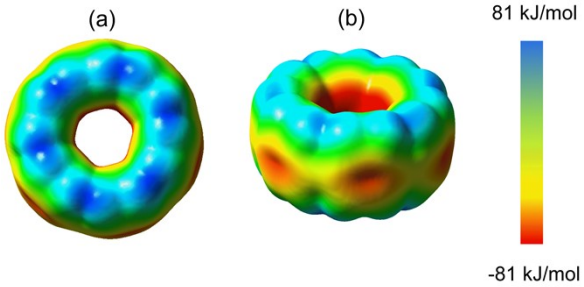

Figure S5. Electrostatic potential map of Cu_7@[6]CPP.

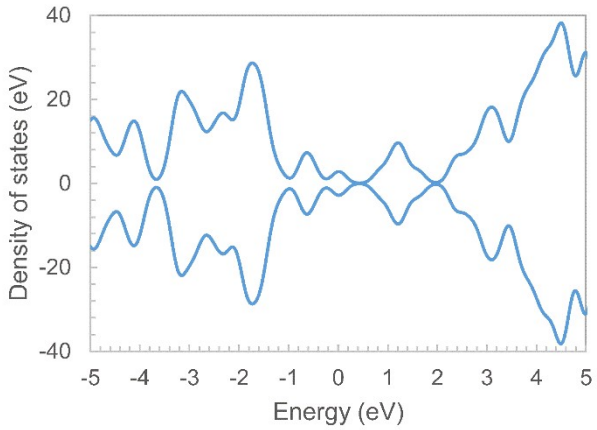

Figure S6. Calculated total density of states of Cu_7@[6]CPP. The Fermi level (E_F) is set to zero.

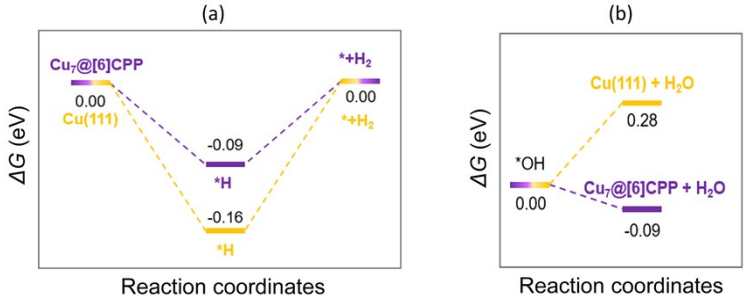

Figure S7. Free energy diagrams of the HER and OH elimination processes on Cu(111) and Cu_7@[6]CPP.

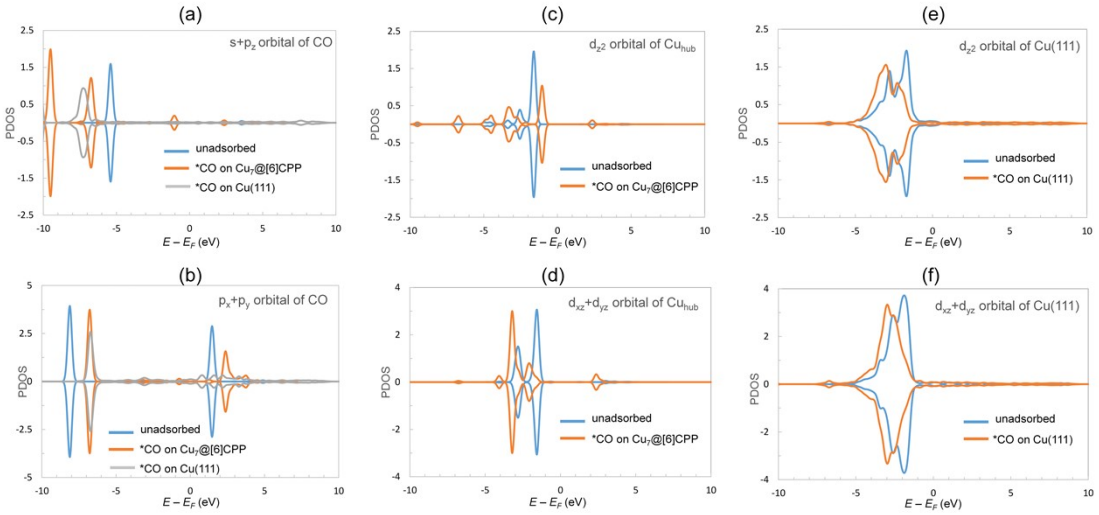

Figure S8. Projected densities of states (PDOS) of CO/*CO and the reacting Cu sites of Cu_7@[6]CPP and Cu(111). The Fermi level (E_F) is set to zero.

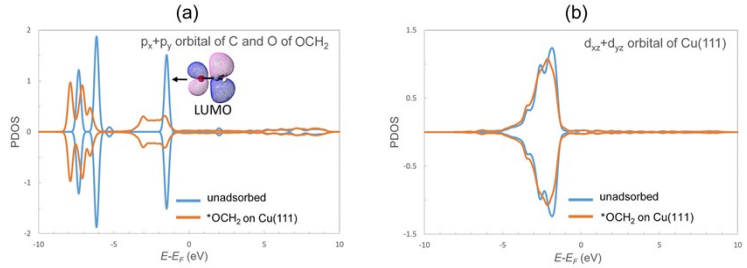

Figure S9. Projected densities of states (PDOS) of OCH_2/*OCH_2 and the reacting Cu sites of Cu(111). The Fermi level (E_F) is set to zero.

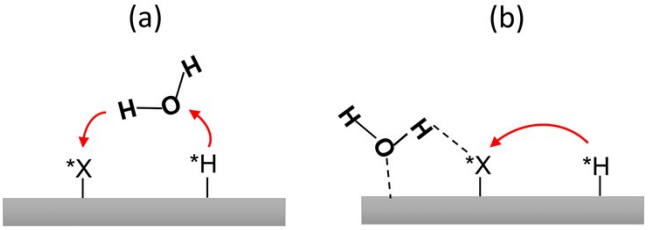

Figure S10. Schematic representations of the (a)H_2O-solvated and (b) H-shuttling models.

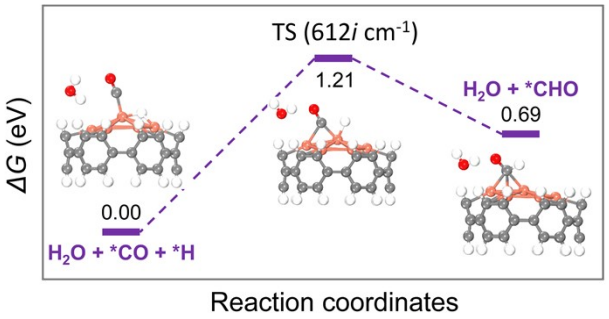

Figure S11. The free energy diagram and relevant structures of the reaction *CO + *H → *CHO along the H_2O-solvated mechanism.

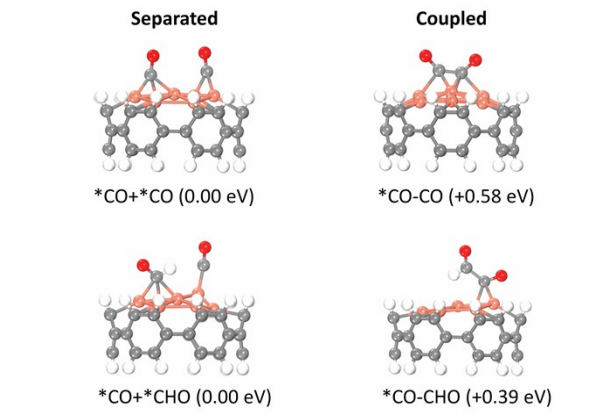

Figure S12. Structures and relative energies of separated and coupled CO-CO and CO-CHO intermediates

Table S1. Calculated energy of optimized Cu_n@[6]CPP structures (n=1-9). (a), (b) and (c) represent different structures with the same number of Cu atoms

Structure	$E_{(a)}$ (eV)	$E_{(b)}$ (eV)	$E_{(c)}$ (eV)
Cu_1@[6]CPP	-409.78	-409.36	
Cu_2@[6]CPP	-412.82	-411.03	
Cu_3@[6]CPP	-415.19		
Cu_4@[6]CPP	-417.61	-417.45	-417.32
Cu_5@[6]CPP	-420.55	-420.47	
Cu_6@[6]CPP	-423.32	-422.94	
Cu_7@[6]CPP	-426.93	-426.21	
Cu_8@[6]CPP	-429.46	-429.36	
Cu_9@[6]CPP	-432.19	-432.16	-431.58

Table S2. Formation energy (E_f) of the most stable structure of Cu_n@[6]CPP (n=1-9)

n	Cu_{n-1}@[6]CPP (eV)	Cu_n@[6]CPP (eV)	Cu (eV)	E_f (eV)
1	-409.00	-409.78	-0.24	-0.53
2	-409.78	-412.82	-0.24	-2.80
3	-412.82	-415.19	-0.24	-2.13
4	-415.19	-417.61	-0.24	-2.18
5	-417.61	-420.55	-0.24	-2.70
6	-420.55	-423.32	-0.24	-2.52
7	-423.32	-426.93	-0.24	-3.37
8	-426.93	-429.46	-0.24	-2.29
9	-429.46	-432.19	-0.24	-2.49

Table S3. The electronic energy (*EE*), free energy correction (CORR, including ZPE, entropy, and solvation corrections), and free energy (*G*) of each relevant structure on the C_1 route of CO reduction catalyzed by Cu_7@[6]CPP

Structure	*EE* (eV)	*CORR* (eV)	*G* (eV)
Cu_7@[6]CPP	-426.90	11.92	-415.00
*CO	-442.51	11.96	-430.55
*CHO	-445.80	12.24	-433.56
Cu_7@[6]CPP + HCHO	-449.24	12.63	-436.61
CO	-14.78	-0.39	-15.17
H_2	-6.77	-0.04	-6.81
HCHO	-22.13	0.13	-22.00
CO_2	-22.95	-0.26	-23.21
H_2O	-14.22	0.09	-14.13

Table S4. The electronic energy (*EE*), free energy correction (CORR, including ZPE, entropy, and solvation corrections), and free energy (*G*) of each relevant structure on the C_1 route of CO reduction catalyzed by Cu(111)

Structure	*EE* (eV)	*CORR* (eV)	*G* (eV)
Cu(111)	-283.09	0.00	-283.09
*CO	-298.82	0.01	-298.81
*CHO	-301.55	0.29	-301.25
*OCH_2	-305.25	0.50	-304.75
*OCH_3	-309.88	0.91	-308.97
*O	-289.68	0.06	-289.62
*OH	-293.91	-0.18	-294.09
CO	-14.78	-0.39	-15.16
H_2	-6.77	-0.04	-6.81
CH_4	-24.04	0.71	-23.32
H_2O	-14.21	0.09	-14.13
CO_2	-22.96	-0.26	-23.21

Table S5. The electronic energy (*EE*), free energy correction (CORR, including ZPE, entropy, and solvation corrections), and free energy (*G*) of implicit H_2O solvation corrected *CO and *CHO on the C_1 route of CO reduction catalyzed by Cu_7@[6]CPP

Structure	*EE* (eV)	*CORR* (eV)	*G* (eV)
*CO	-443.00	12.06	-430.94
*CHO	-446.29	12.35	-433.95